

Processing and structures of bi-phase oxide ceramic filaments

A. Poulon-Quintin^a, M.H. Berger^a, A.R. Bunsell^{a,*}, C. Kaya^b, E.G. Butler^b, A. Wootton^c,
M.H. Lewis^c

^a*Ecole des Mines de Paris, Centre des Matériaux, BP 87, 91003 Evry Cedex, France*

^b*IRC in Materials Processing, The University of Birmingham, Edgbaston, Birmingham B15 2TT, UK*

^c*University of Warwick, Department of Physics, Centre for Advanced Materials, Coventry CV4 7AL, UK*

Received 13 July 2002; received in revised form 26 February 2003; accepted 7 March 2003

Abstract

Two phase ceramic filaments have been made by the co-extrusion of different green mono-filaments, each extruded mono-phase being produced from two differing material sources. The first was based on sol technology and the second based on oxide ceramic powder (+ thermoplastic binder) processing. Initially, mono-phase filaments were produced and re-extruded to produce bi-phase filaments which were then sintered to produce ceramics with aligned fine microstructures. The scale and fineness of the final sintered structure and the orientation of the grains in each phase (alumina or zirconia) have been determined by SEM and TEM and have been found to depend on the type of original precursor used, the powder grain size added and the temperature of heat treatment chosen. The study seems to demonstrate the viability of this novel multiple sol-gel based extrusion process to obtain optimised engineering structures for use at high temperatures. © 2003 Elsevier Ltd. All rights reserved.

Keywords: Al_2O_3 ; Extrusion; Filaments; Microstructure; Sol-gel processes; TEM; ZrO_2

1. Introduction

The need for structural materials capable of operating at temperatures above the limits of advanced metallic super alloys has incited much interest in CMCs reinforced by ceramic fibres. The cost and difficulty of producing fibres capable of resisting exposure at high temperatures in oxidising environments are considerable as is the control of the fibre matrix interface and manufacture of CMC parts. This has prompted a novel route for the development of in situ aligned structural composites by a process involving the co-extrusion of different precursor materials.

Of the many ceramic fabrication techniques available, extrusion is considered to be the most suitable and cost effective method for producing a variety of shapes with constant cross-section. Moreover, the extrusion of viscous pastes has become increasingly important due to the advantages of forming products at low temperatures and pressures.

Because extrusion is based on plastic forming, there exist certain mechanical requirements for extrusion to

occur. The first requirement is flow. The material to be extruded must be plastic (or flowable) enough during the extrusion process to form the desired cross section under the application of pressure. The second requirement is green strength. After the material is extruded, it must be strong enough to resist deformation due to its own weight (slumping) or due to handling stresses. If either of these conditions is not met, good extrusion will not be obtained. Moreover, to co-extrude two green rods of two different phases, the pastes used must have similar rheological behaviour during extrusion. Their shrinkage compatibilities during heat treatment are also necessary which may require further adaptation by the addition of powders of varying particle size. The optimum microstructure sought for the final sintered material would consist of two continuous distinct aligned narrow phases on a micrometer scale. Each phase should itself be composed of aligned and elongated grains to optimise the mechanical properties.

2. Materials

The aim of this study was to understand and compare the final, sintered microstructures of multi-extruded, bi-

* Corresponding author. Tel.: +33-1-60-76-3015; fax: +33-1-60-76-3150.

E-mail address: anthony.bunsell@mat.enscm.fr (A.R. Bunsell).

phased, materials which were made from either sol based or oxide powder based raw materials. The two phases of interest were: α -alumina and yttrium stabilised tetragonal zirconia (Y-TZP).

Filaments obtained by the extrusion of commercially available ceramic powders with a thermoplastic binder were supplied by the University of Warwick to provide model systems for the study of the microstructures of $\text{Al}_2\text{O}_3/\text{ZrO}_2$ co-extruded filaments. The alumina batch powders used for the green monophase filaments were composed of α -alumina A16 supplied by Alcoa (mean particle size, 1 μm) and Ceralox APA 0.5 (0.4 μm) and Dispersal 20/2 (<0.1 μm) supplied by Morgan Material Technology, UK. Zirconia green monofilaments were produced using HSY3B (5.3 wt.% Y_2O_3) powder supplied by Mandoval Ltd. ($\sim 0.75 \mu\text{m}$). The thermoplastic binder used to aid extrusion was a low molecular weight polyethylene supplied by Alpha Chemical Ltd. with a melting point around 115 $^\circ\text{C}$.

Filaments obtained by the extrusion of sol based materials were supplied by the University of Birmingham using material supplied by Morgan Material Technology. Remal A20 boehmite sol was used for the green monophase filaments (Remet Corp., USA (average particle size 50 nm) with additions of ceramic powder seeds of α - Al_2O_3 powder (Baikalox SM8, 250 nm) and zirconia powder (Degussa, Germany, 30 or 150 nm). Zirconia green monophase filaments were produced using a sol based on a very pure zirconia powder (Degussa, VP zirconia) and additions of Remal A20 boehmite sol and Bailalox SM8 α - Al_2O_3 powder.

These starting materials are shown in Table 1.

3. Processing

3.1. Thermoplastic/oxide powder processing

Each oxide powder underwent a shear mixing regime at a temperature around 120 $^\circ\text{C}$ to produce a 50 vol.% containing oxide powder/thermoplastic feed material

for the extrusion process. Oxide powder was added gradually to the preweighted amount of heated thermoplastic and as the oxide solids loading increased, small amounts of polyethyleneglycol (PEG 400) were added to aid fluidity of the melt. As the melt cooled, the thermoplastic solidified and the room temperature oxide powder/thermoplastic mix was used as a feed material for the co-extrusion process.

The extrusion process was a classical process² involving the use of a piston moving in a cylinder, which was heated to aid extrusion through a die. A computer was used to display and store extrusion pressure versus piston displacement so as to control the reproducibility of the extrusion parameters and to give a guide to rheological behaviour under extrusion processing.

A vital processing step was the removal of the thermoplastic wax after extrusion without distortion of the filament structure. Slow heating rates (10 $^\circ\text{C}/\text{h}$) and staged dwell times were essential for a successful burn-out process. Filament sintering up to 1670 $^\circ\text{C}$ (20 $^\circ\text{C}/\text{h}$) produced straight rods of $\sim 3 \text{ mm}$ in diameter.

3.2. Sol based processing

Each of the seeding powders was first dispersed in water and then added into the boehmite sol in order to produce fine-grain ceramics. Glycerol was added in order to minimize the surface roughness of the extruded rods. The final sol was ball milled and then dried in a micro-wave in order to obtain a gel structure. ZrO_2 sols were found to require a vacuum drying step instead of micro-wave drying which produced unwanted agglomerations. The final soft white gel was compacted using filtration apparatus to squeeze out excess water. Seeded sols were successfully extruded using a die apparatus. Straight rods 2 mm in diameter were obtained, dried on a grooved plate to maintain straightness and then sintered to different selected temperatures from 1450 to 1550 $^\circ\text{C}$. As for the oxide powder/thermoplastic extrusion technique, sol paste rheology was monitored during extrusion (load applied versus piston position) using a

Table 1
Starting materials used for co-extrusion

Sol- gel route				Thermoplastic/oxide powder processing		
		Suppliers	Powder grain size		Suppliers	Powder grain size
<i>Alumina phase</i>				<i>α-Alumina phase</i>		
	Boehmite sol	Remet. Corp.	50 nm	α -alumina A16	Alcoa	1 μm
	Remal A20	USA				
Seeds	α -alumina Baikalox SM8	Degussa	250 nm	Ceralox APA0.5	MMT	0.4 μm
		Germany			UK	
	ZrO ₂	Degussa	30 or 150 nm	Dispersal 20/2	MMT	<0.1 μm
		Germany			UK	
<i>Zirconia phase</i>				<i>Zirconia phase</i>		
Seeds	VP zirconia	Degussa Germany	30 nm			
	Boehmite sol Remal A20	Remet. Corp. USA	50 nm	HSY3B	Mandoval Ltd	0.75 μm
	α -alumina Baikalox SM8	Degussa Germany	250 nm			

computer linked to the testing machine. This allowed preferential water migration during extrusion due to the non homogeneous water concentration within the sol paste after filter pressing to be controlled.

3.3. Co-extrusion process

The multi-extrusion process principle was the same for each type of extruded green filaments only the die apparatus was different: with heating for the thermoplastic/oxide powder processing (cf. Section 3.1) and at room temperature for the sol gel route (cf. Section 3.2). The green single phase filaments were first extruded, then combined so as to be co-extruded and the bi-phased filament obtained once again re-extruded to reduce the widths of the phases,¹ as shown in Fig. 1.

One advantage of multi-extrusion is that different diameters can be used for each phase so that different volume ratios of each phase inside the final bi-phased filament can be obtained. Sintering without distortion of the filament structure and without the creation of cracks at the interfaces between two phases are a vital processing step depending on the rheology of the paste, the seeding powders used, the die geometry and the extrusion filament speed.

3.4. Experimental testing procedure

The filament porosities were observed using a ZEISS AXIOVERT 405M optical microscope and a LEO DSM982 Gemini FEG.

The effects of multi-extrusion on the microstructure were investigated using a PHILIPS EM430 TEM-STEM with an acceleration voltage of 300 kV. Particular attention was paid to the diffusion of elements from one phase to the other as well as the quality of

the interface between two different filament phases. A “tripod” wedge polisher was used to prepare the thin foils which during the final stage were ion milled for 2 h.

The mechanical behaviour of the filaments was studied at room temperature using three-point bending test. The sample sizes used were ~ 3 mm in diameter with a span length of 18 mm for the powder based filaments and was ~ 2 mm in diameter with a span length of 20 mm for the sol-gel based filaments.

4. Results

4.1. The alumina-based mono-filaments

For each type of filament, optical observations of a polished sections of filaments parallel to the extrusion direction revealed that the process of extrusion led to partially oriented porosity, as shown in Fig. 2, aligned with the extrusion direction and larger than the random inter or intragranular oriented porosity which was more or less spherical. The size of this oriented porosity depended on the technology used (sol or powder) and the paste rheology. Moreover, cross sections of powder based filaments revealed cracks radiating from the filament centre. These may have appeared during thermoplastic burnout.

For the sol-gel based materials, it was observed that filaments from an un-seeded boehmite sol-gel consisted of a very porous vermicular microstructure even when high sintering temperatures were used (1650 °C). To overcome this and to control grain size and intergranular porosity of the extruded filament, the alumina sol was seeded with powder additions (5–10 wt.%) of α -alumina (250 nm) or zirconia (30 or 150 nm) which allowed a fine and dense microstructure to be obtained

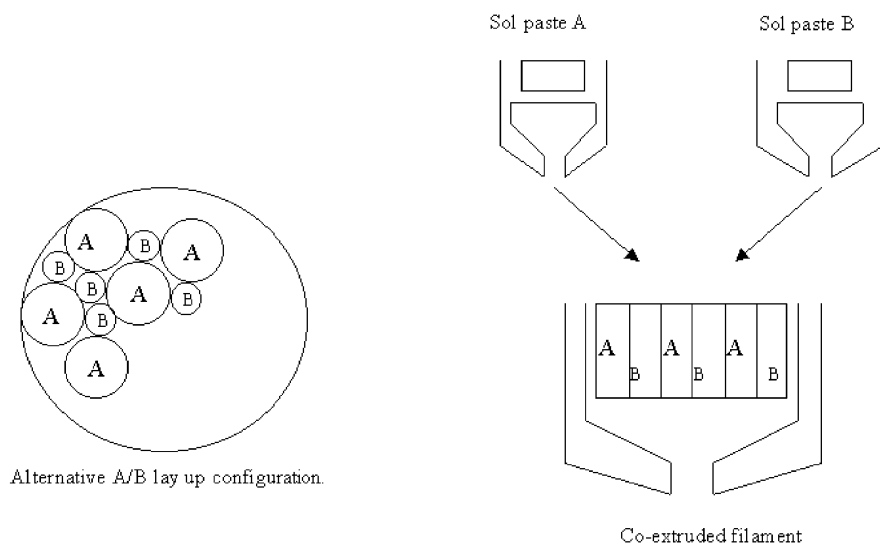


Fig. 1. Schematic of the multi-extrusion process.

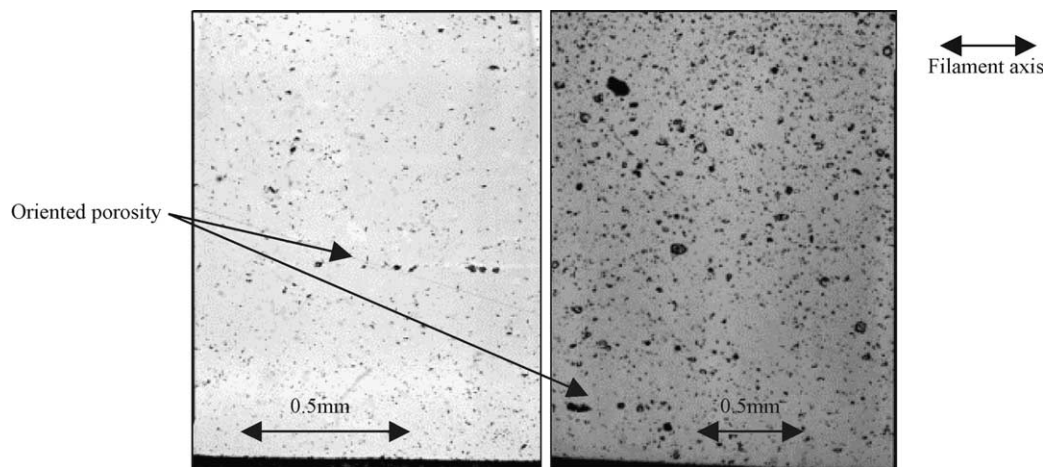


Fig. 2. Optical micrograph of the partially oriented porosity inside Boehmite + α -alumina (sol) and α -alumina filaments (powder).

at the lowest possible temperature.³ At a sintering temperature of 1450 °C the addition of α -alumina powder allowed α -alumina grains of 4 μm in size to be obtained whereas the addition of zirconia seeds led to a reduction of the α -alumina grain size ($\sim 2 \mu\text{m}$), as shown in Table 2. Seeding produced a more homogeneous grain size distribution and resulted in isotropic microstructures with no particular grain orientation parallel to the fibre axis (cf. Fig. 3). An increase in sintering temperature led to increase alumina grain size regardless of the powder seed added.

Table 2
 α -Alumina average grain size inside alumina based filaments

		Heat treatment temperature	α -Alumina average grain size (μm)
Sol-gel	Boehmite	1450 °C, 2 h	4
	+ α -alumina	1500 °C, 2 h	4.5
		1550 °C, 2 h	5
	Boehmite	1450 °C, 2 h	2.3
	+ zirconia	1500 °C, 2 h	3
		1550 °C, 2 h	3.2
Powder	α -alumina	1670 °C, 2 h	10

Compared to the sol based process, the powder based technology showed a less dense microstructure after higher heat treatment temperatures. The alumina grain size was two to three times greater than for the previous materials. No particular microstructure aligned parallel to the fibre axis was noticed (cf. Fig. 3).

Three-point bending test results are summarized in Table 3. An increase in the heat treatment temperature, which led to an increase of α -alumina grain size, led to a decrease of the failure strength. The strongest filaments were the boehmite + α -alumina sol-gel based material. The presence of radial cracks explains the low mechanical behaviour of the material obtained by the powder based process. The presence of larger porosities due to the paste rheology inside the zirconia seeded alumina based filaments explain the lower strength compared to the α -alumina seeded filaments and the different failure modes.

4.2. The zirconia-based mono-filaments

On an optical scale, the porosity in these two types of zirconia based filaments was comparable to that of the alumina based filaments but was more spherical in

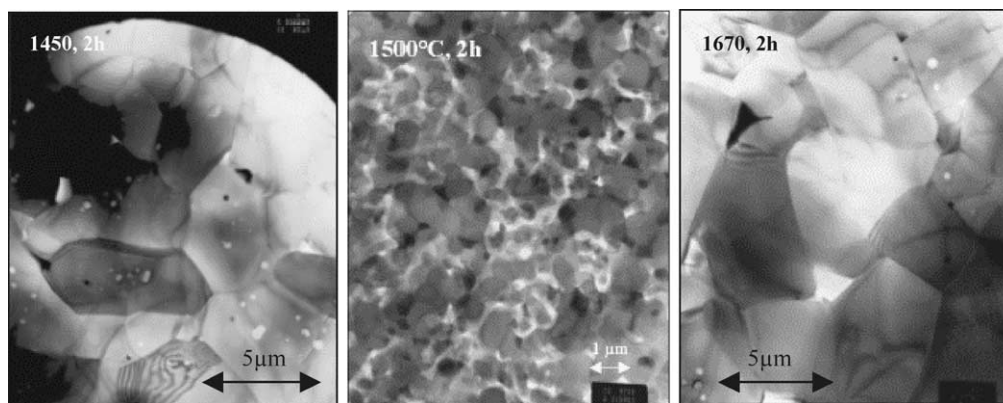


Fig. 3. TEM micrographs of α -alumina based filaments. Left: Boehmite + α -alumina (1450 °C, 2 h), middle: boehmite + zirconia (sol-gel process, 1500 °C, 2 h) and right: α -alumina (powder based process, 1670 °C, 2 h).

Table 3
Three point bending test results for alumina based monofilaments

	Heat treatment temperature	Failure strength (MPa)	Failure mode
Boehmite + α -alumina	1450 °C, 2 h	520±60	Mostly intragranular
	1500 °C, 2 h	500±100	
Boehmite + zirconia	1500 °C, 2 h	360±30	Mostly intergranular
	1550 °C, 2 h	245±60	
α -Alumina	1670 °C, 2 h	300±50	Mixed mode

shape. TEM micrographs showed a fully dense microstructure after a heat treatment at 1400 °C for 3 h. The effect of an increase in the sintering temperature led to an increase of both the alumina and the zirconia grain sizes in different proportions, as can be seen from Table 4. Many zirconia grains were twinned and large grains of alumina were observed around pores for sol based filaments. The powder based filaments were less dense and showed large cracks and pores, as was noticed for the alumina based filaments. These zirconia filaments enclosed randomly oriented twinned and un-twinned zirconia grains presenting an average grain size larger than those inside the sol-gel based filaments, as shown in Fig. 4.

Three-point bend test results are summarized in Table 5. The strongest materials were the sol based filaments. Radial cracks can explain the difference between failure strength values found for sol and powder based

specimens. As for alumina filaments, the values obtained can be attributed to the presence of areas of high porosity which also induced different failure modes.

4.3. The multi-extruded filaments

4.3.1. Microstructure of the powder based co-extruded filaments

Fig. 5 shows optical micrographs of the co-extruded powder based filaments. For these bi-phase materials two kinds of porosity were present. The first was dispersed evenly inside the filaments and its extent depended on the volume ratio of the zirconia used. The second consisted of large pores usually located inside the alumina phase whatever the alumina/zirconia volume ratio employed. Large cracks may have appeared during burnout of the thermoplastic as well as pores similar to those observed in the mono-filaments. Sintered microstructures of a 50/50 vol.% alumina/zirconia co-extruded filament showed large crack pathways surrounding individual filaments or following the boundary of an interface. Rheological differences between the two phases during extrusion coupled with differential burnout and sintering shrinkages explained the existence of these non-contact areas. A proposed solution to minimise rheological distortion was to change the volume percentage distribution of the two phases.

Table 4
Zirconia and α -alumina average grain sizes inside zirconia based filaments

	Heat treatment temperature	Zirconia average grain size (μm)	α -Alumina average grain size (μm)
Zirconia sol based	1350 °C, 3 h	0.3	0.4
	1400 °C, 3 h	0.4	0.5
	1450 °C, 3 h	0.5	0.9
Zirconia powder based	1670 °C, 2 h	0.5	3

Table 5
Three point bending test results for zirconia based monofilaments

	Heat treatment temperature	Failure strength (MPa)	Failure mode
Sol	1350 °C, 3 h	865±60	Mostly intergranular
	1400 °C, 3 h	934±60	
	1450 °C, 3 h	859±60	
Powder	1670 °C, 2 h	316±150	Mixed mode

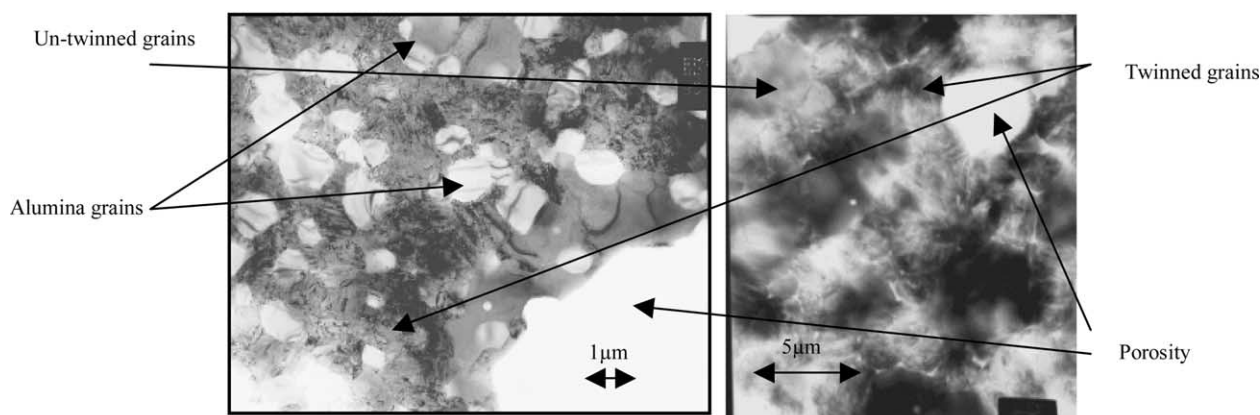


Fig. 4. TEM micrographs of sintered, ZrO_2 monofilaments. (left) sol based (1500 °C/3 h), and (right) powder based (1670 °C/2 h).

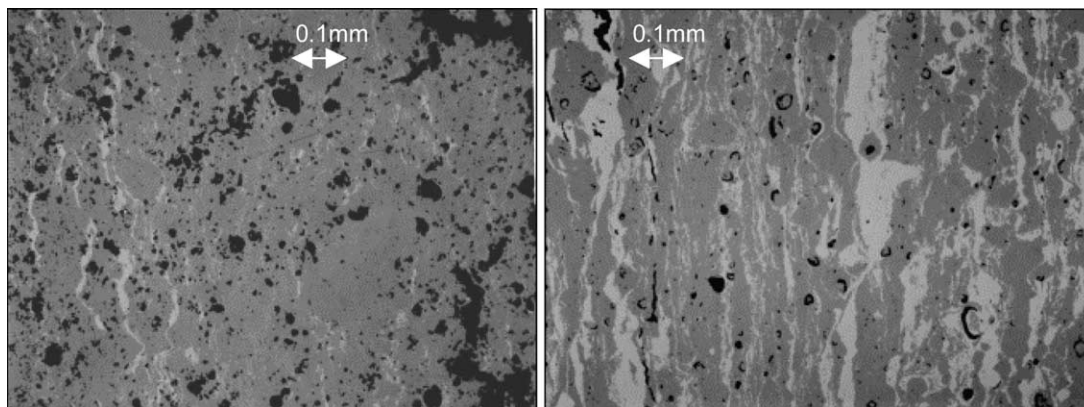


Fig. 5. Optical micrographs of co-extruded powder based filaments of: 98.8/1.2 vol.% (left) and 77/23 vol.% (right) both sintered at 1670 °C.

For a volume ratio of 98.8/1.2 vol.% $\text{Al}_2\text{O}_3/\text{ZrO}_2$, zirconia micro-fibrils were found to be aligned parallel to the filament axis but were not uniformly dispersed inside the filament and were corrugated in shape. Their widths were less than 30 μm . TEM observations showed that the size of alumina grains were not modified by the presence of zirconia fibrils (alumina average grain size 10 μm). At higher magnifications, the very thin fibrils (<10 μm) were seen to be discontinuous and zirconia grains seemed to be dispersed between alumina grains.

For a volume ratio of 77/23 vol.% $\text{Al}_2\text{O}_3/\text{ZrO}_2$, the width of the zirconia fibrils varied from 1 to 100 μm . At low magnification ($\times 5$), the fibrils seemed to be straight and more or less continuous but as the magnification was increased some discontinuities and wavy interfaces were revealed. TEM observations, shown in Fig. 6, showed that for fibril widths of a few microns, the growth of the alumina grains was restricted to $\sim 2 \mu\text{m}$ whereas inside wide alumina fibrils (100 μm) the grain size (8 μm) was similar to that of the alumina monofilaments.

A study of the interfaces between fibrils of different phases revealed neither cracks nor elongated alumina

grains for both kinds of co-extruded filaments. EDX analysis did not reveal interdiffusion between the two phases. No yttrium and no zirconium was found at the alumina/alumina grain boundaries. Moreover, no silicate phase was noticed.

The failure strength of alumina/zirconia 77/23 vol.% $\text{Al}_2\text{O}_3/\text{ZrO}_2$, shown in Table 6, was higher than the value for both of the monofilaments and the 98.8/1.2 volume ratio used. The fracture morphology of a co-extruded 77/23 vol.% $\text{Al}_2\text{O}_3/\text{ZrO}_2$ is shown in Fig. 7. For the 77/23 filaments, the failure mode was intragranular for the alumina phase and mixed for the zirconia phase. The failure surfaces of the 98.8/1.2 composition, showed intragranular crack propagation in both phases with several cracks being observed radiating from the centre of the filament.

Table 6

Three point bending test results for powder based filaments

Final volume ratio (alumina/zirconia)	Failure strength (MPa)
77/23	360 \pm 60
98.8/1.2	130 \pm 30

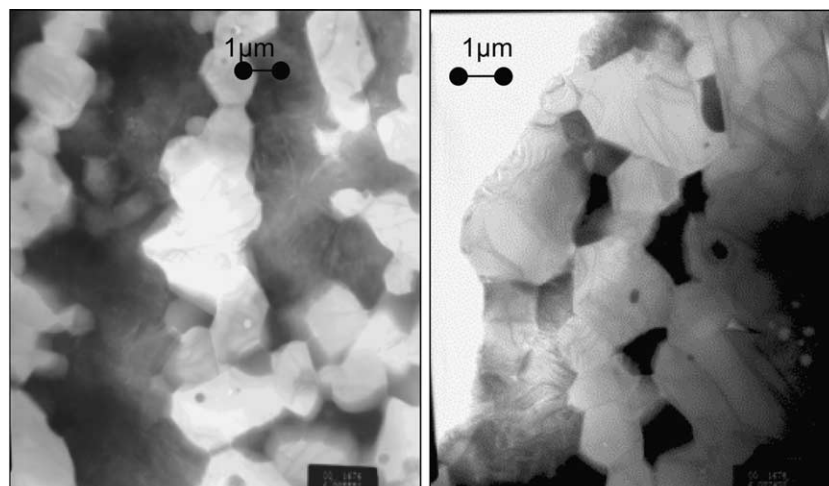


Fig. 6. TEM micrographs of a co-extruded powder filament (77/23 vol.%) sintered at 1670 °C.

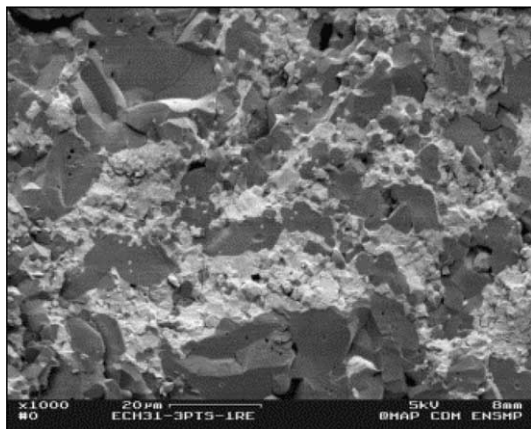


Fig. 7. SEM micrograph of the fracture morphology of a co-extruded (77/23 vol.%) filament (powder).

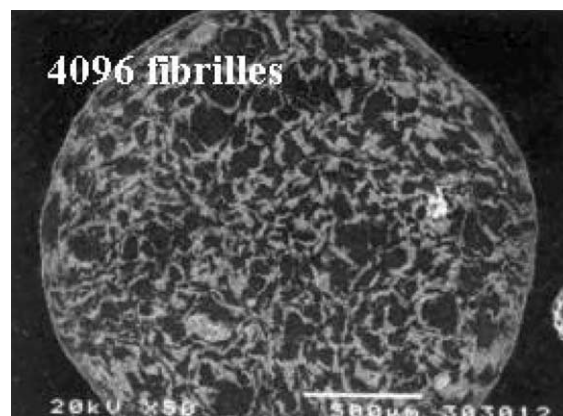


Fig. 8. SEM micrograph of the sintered (1450 °C, 3 h) 3 times co-extruded boehmite/zirconia sample showing the fibrils size and homogeneous distribution of the fibrils.

4.3.2. Microstructure of the sol based co-extruded filaments

Two kinds of sintered bi-phased filaments were supplied by the University of Birmingham based on the results obtained on the different mono-phased filaments: Boehmite + α -Al₂O₃ / ZrO₂ + 10 wt.% α -Al₂O₃ (1500 °C, 3 h), and Boehmite + α -Al₂O₃/ZrO₂ + 5 wt.% zirconia powder (1500 °C, 3 h). The initial composition of the zirconia phase had been changed because of un-desired microstructure after co-extrusion (the initial form of the mono-filaments was not conserved) and differential shrinkage during sintering. These two compositions presented the same rheological properties (same behaviour during extrusion). These two compositions were comprised of the 30 nm Degussa ZrO₂ sol with additions of 10 wt.% α -Al₂O₃ and 5 wt.% 200 nm ZrO₂ as seed materials. For co-extrusion, a volume ratio of 50/50 vol.% was used which was obtained with 8 square monofilaments of each phase placed together in a square array. After the third co-extrusion each filament contained 4096 (16³) fibrils, homogeneously distributed within the final microstructure, as shown in Fig. 8. No cracks at the interfaces after sintering were observed after sintering.

Optical microscope observations, shown in Fig. 9, showed that the width of the phases were not regular and that the interfaces were more or less aligned with the filament axis but not straight. The porosity was confined in the alumina fibrils. Transverse cracks inside the zirconia phase appeared during polishing which is characteristic of a highly pre-constrained structure. The microstructural characteristics of these materials are summarized in Table 7. TEM observations showed that the average grain size of the alumina was unchanged inside areas of large phase width (100 μm). For the ZrO₂ + 10 wt.% α -Al₂O₃ zirconia mono-filament composition, there was no particular orientation of the grains with alumina grains usually being of random size and shape whereas for the ZrO₂ + 5 wt.% ZrO₂ zirconia

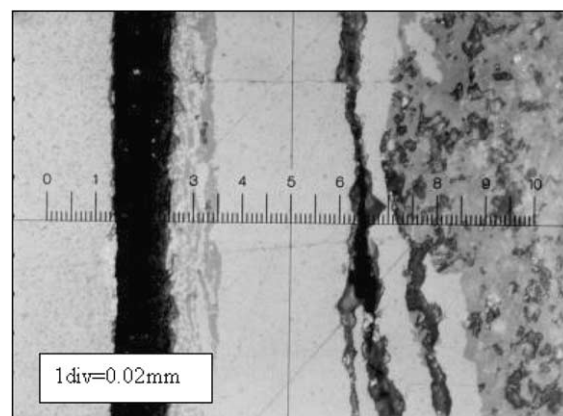


Fig. 9. Optical micrograph of the sintered (1450 °C, 3 h) 3 times co-extruded boehmite/zirconia sample showing the fibrils size on a longitudinal section.

mono-filament composition, elongated alumina grains were found parallel to the interface, as shown in Fig. 10, depending on the width of the alumina phase observed.

EDX analysis of alumina/alumina boundaries close to the interface with a zirconia fibril showed a significant silicon peak, particularly at the triple points, as shown in Fig. 11. The presence of an amorphous intergranular silicate phase was confirmed by a characteristic diffuse ring on the electron diffraction pattern.

The failure strengths of the filaments containing ZrO₂ + 5 wt.% ZrO₂ zirconia mono-filaments were the highest. The failure modes of the co-extruded filaments were intragranular for the zirconia phase and mixed inside the alumina phase with a majority of intragranular fractured grains. However, the expected deviation of the cracks at the alumina/zirconia fibril interfaces during three-point bend test at room temperature was not observed, as is revealed in Fig. 12 which shows an interface between the alumina and zirconia phases on a failure surface.

Table 7
Microstructural characteristics of the co-extruded sol based filaments

Composition	Boeh/zirconia + 10 wt.% α -alumina	Boeh/zirconia + 5 wt.% zirconia
Heat treatment	1500 °C, 3 h	1500 °C, 3 h
Grain size		
Alumina	1–10 μm	1–10 μm
Zirconia	0.5 μm	0.5 μm
Width of the phases (nm)		
Alumina	0.25	0.3
Zirconia	0.2	0.1
Elements at the alumina/ alumina boundaries (EDX)	Zr, Si	Zr, Y, Si

5. Discussion

The role of seeding⁴ is known to lower phase transformation temperatures, enhance densification rates and refine microstructures. For the alumina sol based fila-

ments, as the sintering temperature was increased, a decrease in strength was recorded showing that there was significant grain growth at high sintering temperatures which was in agreement with the microstructural results. As well as growth of α -alumina grains, the quantity of intragranular and intergranular porosity also increased. The maximum three-point bending strength (520 MPa) was recorded for alumina seeded filaments sintered at 1450 °C for 2 h. Zirconia seeding also improved the mechanical properties of boehmite based filament as the alumina grain size is reduced because zirconia acts as a grain growth inhibitor for alumina grains, although porosity was observed to increase which resulted in the maximum strength value obtained being lower than that of the alumina seeded material. From these observations, it was clear that α -alumina seeding was the most suitable technique to promote and control the θ - to α -alumina transition, resulting in high densification and

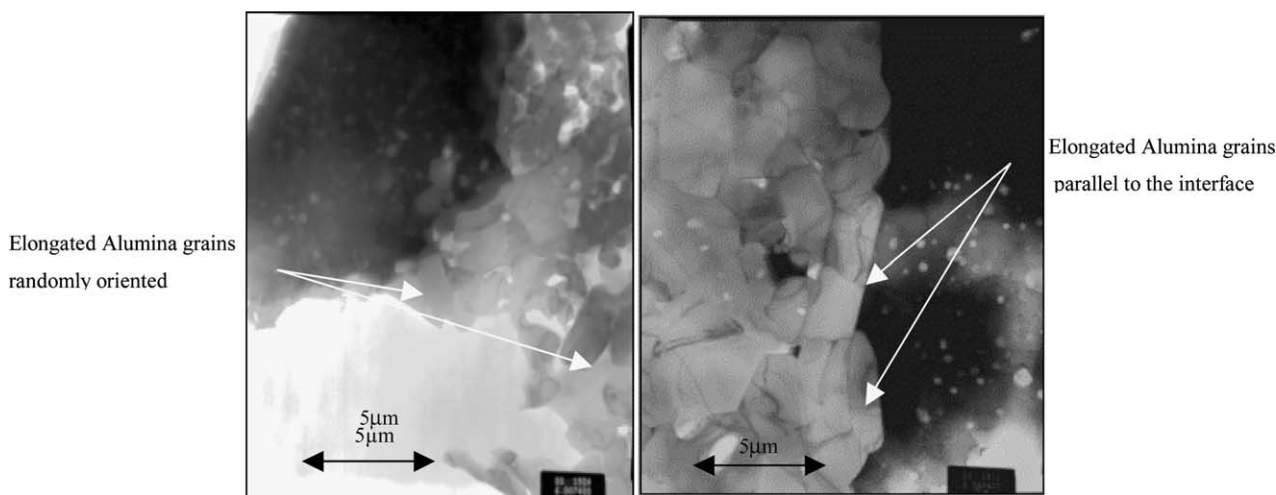


Fig. 10. TEM micrographs of sol based interfaces; (left) Boehmite + α -alumina / ZrO_2 + α -alumina and (right) Boehmite + α -alumina / ZrO_2 + zirconia.

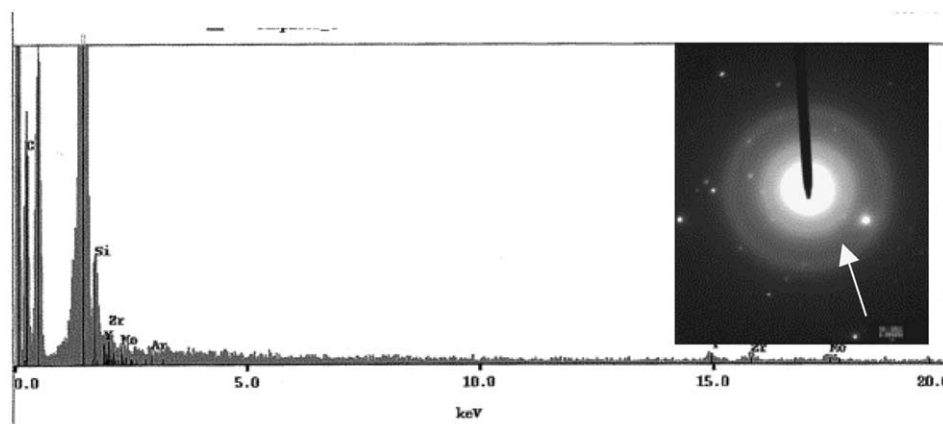


Fig. 11. EDX spectrum of a triple point inside the alumina phase and corresponding electron diffraction pattern (sol based).

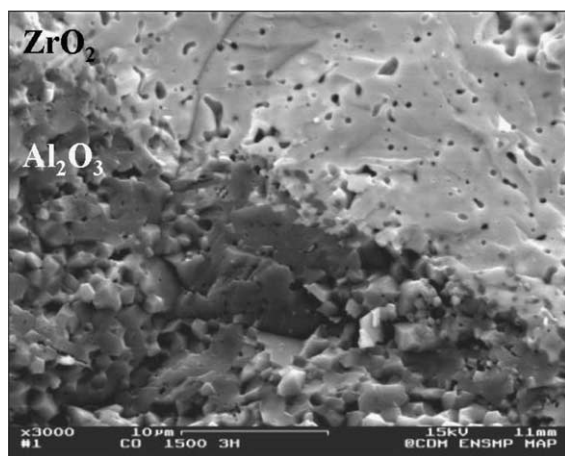


Fig. 12. Detail of failure surface after a three point bend test at room temperature (boehmite + α -alumina / ZrO_2 + zirconia, 1500 °C, 3 h).

good flexural strength. These observations also explained why the mechanical strengths of the alumina powder based filaments were lower as the alumina grain sizes were twice as large as those obtained with -alumina seeding which contained a large amount of porosity.

For the zirconia sol based filaments, lowering the sintering temperature increased the density of the final filament. Very fine alumina seeded boehmite particles precipitated either within the zirconia grains or at grain boundaries and at triple junction of zirconia grains. The microstructure was fully dense. Just as zirconia seeds are alumina grain growth inhibitors, alumina seeds inhibit growth of zirconia grains.⁵ Due to the nano-ceramic nature of the final sol based ZrO_2 filament both the toughness and strength values were high. The huge difference in the values of failure strengths obtained by the two processes can be explained by porosity as the zirconia and alumina grain sizes were of the same order. Moreover, the different modes of failure observed were linked with the presence of alumina grains.

For the co-extruded materials, with an unmodified sol based ZrO_2 composition, extensive crack formation was observed at the interfaces after sintering due to differences in shrinkage during sintering between the two co-extruded phases. Cracking could be eliminated by the addition of α -alumina⁶ or 200 nm zirconia in the sol based ZrO_2 composition by altering shrinkage rates. However, these additions changed the sol rheology which was adjusted by modifying the amount of cyclohexanone addition.

Microstructural changes observed with the 200nm zirconia addition to the sol based ZrO_2 were that the main zirconia matrix contained sub-micron grains and also large zirconia grains. Alumina powder additions produced no noticeable microstructural changes except

for an increase in the proportion of alumina grains. The porosity inside the sol based extruded mono-phased materials was more or less uniformly dispersed inside the filaments except for the partially oriented porosity which did not present a regular distribution inside the filament. For the bi-phased filaments, the multi-extrusion process seemed to reduce porosity due to processing and to preferentially confine it to the alumina phase. The effect of multi-extrusion on grain size was less obvious inside the sol-gel based filaments. Contrary to the powder based materials no particular differences were noticed in alumina grain size if the grains were localised inside a fine or a large fibril.

In both kinds of materials, the number of effective co-extrusions was limited to three. After three co-extrusions (giving a phase width of approx 100 μm), the fibrils were no longer continuous and zirconia grains appeared to be dispersed inside the alumina matrix. The starting powder grain size limited the powder based technology by limiting the width of the fine phase. On an optical scale, this technology presented a more constant width of phase even if better fibril linearity and continuity was obtained with the sol based technology. On a micron scale, the quality of the interfaces was controlled by the alignment of the alumina grains with the filament axis. Where the fibrils were distorted, grain alignment was difficult to discern.

Interfaces were straighter when the alumina grains at the interfaces were rectangular. This kind of microstructure was seen with the sol-based technology which allowed a better control of grain growth both in size and shape. However, no particular orientation of the boundaries at the interface between the two phases were noticed even if the alumina basal plane seemed to have an important role when the alumina grains are rectangular shaped.

The behaviour of the cracks at the interfaces directly depends on the interface properties and the existence of orientation relationships between alumina and zirconia grains, modifying the energy of the grain boundaries. Crack bifurcation is not allowed by these interfaces for which de-cohesion is difficult due to strong and stable bonds between the two phases.⁷

6. Conclusion

The results demonstrate the viability of the sol-gel multiple extrusion process in order to obtain engineering bi-phase microstructures for use at elevated temperatures. The desired conditions of aligned microstructure, polycrystalline phases and linear interface between the phases were obtained. The sol based process allowed a better control of final microstructure than the powder based process and it was shown that materials with good mechanical properties could be

improved with a better control of porosity. However, the presence of an intergranular silicate phase observed in TEM could be expected to affect the creep behaviour of the material at high temperatures. The composition of the boehmite sol used had to be modified to decrease its silicate content.

The most impressive advantage of this technology was the total control of the rheology of the different pastes which is the main requirement for successful co-extrusion and for obtaining a good sintered microstructure. The alignment and the symmetry of the two phases combined with good quality interfacial integrity suggests that materials with favourable high temperature properties could be achieved using this process.

Acknowledgements

The authors would acknowledge Y. Favry for their advises on mechanical tests on filaments. This work was supported by European Union contract EXPROC No. BRPR-CT97-0609.

References

1. Kumar, C. S., Hareesh, U. S., Pai, B. C., Damodaran, A. D. and Warriar, K. G. K., Aqueous extrusion of alumina–zirconia (12% ceria) composite using boehmite as extrusion aid. *Ceramics International*, 1998, **24**, 583–587.
2. Terpstra, R.A., Pex, P.P.A.C. and de Vries, A.H. *Ceramic Processing*, Chapman & Hall, 1995.
3. Kermel, C. and Moeltgen, P., Influence of seed nature and content on the microstructure development of sol-gel α -Al₂O₃. *Conference & Exhibition of the European Ceramic Society*, 1999, **1**, 227–228.
4. Radonjic, L. and Nikolic, L., Microstructural and sintering behaviour of magnesia doped, seeded, different boehmite derived alumina. *Ceramics International*, 1999, **25**, 567–575.
5. Lange, F. and Hirlinger, M., Grain growth in two-phase ceramics: Al₂O₃ inclusions in ZrO₂. *J. Am. Ceram. Soc.*, 1987, **70**(11), 827–830.
6. Cai, P. Z., Green, D. J. and Messing, G. L., Constrained densification of alumina/zirconia hybrid laminates, I: experimental observations of processing defects. *J. Am. Ceram. Soc.*, 1997, **80**(8), 1929–1939.
7. Poulon-Quintin, A. Comportement Mécanique et Microstructure de Filaments Céramiques Alumine-Zircone pour applications à haute température. PhD thesis, Ecole des Mines de Paris, France, 26 April, 2002.